Combined infernal and Kelvin-Helmholtz like instabilities in tokamaks with strongly sheared toroidal plasma flows

C. Wahlberg,[1] J. P. Graves[2] and I. T. Chapman[3]

[1]*Department of Physics and Astronomy, EURATOM/VR Fusion Association, P.O. Box 516, Uppsala University, SE-751 20 Uppsala, Sweden*
[2]*Centre de Recherches en Physique des Plasmas, Association EURATOM-Confederation Suisse, EPFL, 1015 Lausanne, Switzerland*
[3]*EURATOM/CCFE Fusion Association, Culham Science Centre, Abingdon, Oxfordshire OX14 3DB, United Kingdom*

Introduction The combination of a low-shear magnetic field and significant toroidal plasma flows is a common feature of many tokamak experiments, especially in spherical tokamaks. It is well known that global, ideal MHD instabilities resonant with the magnetic field in the low-shear region of such plasmas ($m/n \approx q$), so-called infernal or, in the case $m = n = 1$, quasi-interchange (QI) instabilities, can grow in static equilibria of this kind [1]. With the effects of the plasma flow taken into account, however, the MHD stability picure is modified a great deal. Thus, while such flows with a broad radial profile, and weak flow shear, generally have a stabilising effect on infernal and QI instabilities [2], strong flow shear instead enhances the drive of these instabilities through the total effective pressure gradient (static plus dynamic pressure determines the Shafranov shifted toroidal equilibrium). In the limit of a Heaviside step in the radial velocity profile, the instability has the character of a global Kelvin-Helmholtz (KH) instability, peaking at the position of the step, and existing above a threshold rotation frequency [3]. In the present work we use MHD theory for low-shear tokamak plasmas with large aspect ratio and sonic toroidal flows [4] in order to improve the analytical understanding of this KH like instability. We also compare predictions from the analytical theory with numerical code calculations.

Analytical model Assuming isothermal flux surfaces of a toroidally rotating tokamak plasma, the density varies on these surfaces as $\rho(r,\theta) = \rho_0(r)e^{\mathcal{M}^2(R^2/R_0^2-1)}$, with a similar expression valid for the pressure $p(r,\theta)$ [2]. Here, (r,θ,φ) are flux coordinates, R is the major radius, $\mathcal{M} = (\rho\Omega^2R_0^2/2p)^{1/2} \sim 1$ the sonic Mach number and Ω the rotation frequency. The ideal MHD stability equation for such a plasma with large aspect ratio ($\varepsilon = r/R \ll 1$), circular cross section, a beta value of order ε^2, and an extended region of low magnetic shear where $m/q - n \sim \varepsilon$ (generalisation of the infernal mode ordering $m/q - n \sim \varepsilon$ will be discussed in Ref. 6 for the case of a large effective pressure gradient) has the form [4]

$$\left(\mathcal{L}_{m,n} + \mathcal{T}_{m,n}\right)\xi_{m,n} + r^2(m^2 - n^2)\frac{d\tilde{\beta}_0}{dr}\xi_{m,n} - m^2\frac{d\tilde{\beta}_0}{dr}C_+r^{m+1} = 0 \qquad (1)$$

$\xi_{m,n}(r)$ above is the main harmonic of the radial component of the plasma perturbation $\boldsymbol{\xi}$, with angular- and time-dependence $e^{i(m\theta-n\varphi-\omega t)}$ and $\tilde{\beta}_0(r) = 2\mu_0(p_0 + \rho_0\Omega^2R_0^2/2)/B_0^2$ the total

beta value of the plasma, including the contribution from the plasma flow. Furthermore, $\mathcal{L}_{m,n} \equiv d[r^3(m/q-n)^2\, d/dr]/dr - r(m^2-1)(m/q-n)^2$ is the cylindrical tokamak operator and $\mathcal{T}_{m,n} \equiv d(r^3 A_1\, d/dr)/dr + r^2\, dA_2/dr - r(m^2-1)A_1$ the inertia operator, with the coefficients $A_{1,2}$ given by [4]

$$A_1 = -\frac{\omega_D^2-\Omega^2\mathcal{M}^2}{\omega_A^2} - \frac{4q_r^2\omega_D^2(\omega_s^2+2\Omega^2)+\Omega^4}{2\omega_A^2(\omega_s^2-q_r^2\omega_D^2)} = \frac{(\omega_D^2-\omega_{\mathrm{GAM1}}^2)(\omega_D^2-\omega_{\mathrm{GAM2}}^2)}{\omega_A^2(\omega_s^2-q_r^2\omega_D^2)} \tag{2a}$$

$$A_2 = -\frac{\omega_D^2+\Omega^2[(m^2-1)\mathcal{M}^2+2m^2-n^2-4]}{\omega_A^2} + \frac{2mq_r\omega_D\Omega(2\omega_s^2+\Omega^2)}{\omega_A^2(\omega_s^2-q_r^2\omega_D^2)} - \frac{4(q_r^2\omega_D^2+2\Omega^2)\omega_s^2+\Omega^4}{2\omega_A^2(\omega_s^2-q_r^2\omega_D^2)} \tag{2b}$$

Here $q_r = m/n$, $\omega_D = \omega + n\Omega$, $\omega_A^2 = B_0^2/(\mu_0\rho_0 R_0^2)$, $\omega_s^2 = \Gamma p_0/(\rho_0 R_0^2)$, Γ is the adiabatic index and $\omega_{\mathrm{GAM1,2}}$ are the frequencies of the two geodesic acoustic modes (continuum modes) existing at the resonant surface $q = q_r$ of the rotating plasma [4].

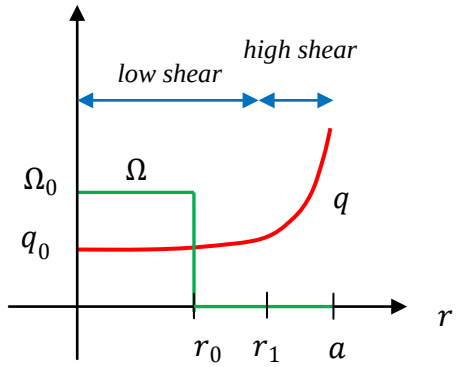

Fig. 1. *Profiles of rotation frequency and safety factor (schematic) in the step model equilibrium*

In order to simulate a situation with locally very strong rotation shear within an extended region of low magnetic shear, we consider a "step model" equilibrium with $\Omega = \Omega_0 = \mathrm{const}$ for $r \le r_0$ and no flow outside $r = r_0$. The magnetic shear $s = rq'/q$ is assumed to be very small in the region $r < r_1$, where $r_0 < r_1$, and finite ($s \sim 1$ or larger) in the edge region $r_1 \le r \le a$ of the plasma. See Fig. 1. Assuming, for simplicity, that $q(r)$, $p_0(r)$ and $\rho_0(r)$ are uniform within the low-shear region $0 \le r \le r_1$, the solution to Eq. (1) in the two regions $0 \le r \le r_0$ and $r_0 \le r \le r_1$ is given by

$$\xi_{m,n}(r) = \left(\frac{r}{r_0}\right)^{m-1}\hat{\xi} \quad \text{and} \quad \xi_{m,n}(r) = \frac{\lambda\hat{\xi}}{\lambda-1}\left[\left(\frac{r}{r_0}\right)^{m-1} - \frac{1}{\lambda}\left(\frac{r_0}{r}\right)^{m+1}\right] \tag{3a, b}$$

respectively, where $\hat{\xi} = \xi_{m,n}(r_0)$ and $\lambda = (r_0/r_1)^{2m}$. $\xi_{m,n}(r)$ above is continuous at $r = r_0$, satisfies the boundary condition $\xi_{m,n}(r_1) = 0$ and is regular at the axis. It is seen that the solution in Eq. (3) peaks at the point of maximum (infinite) rotation shear, and becomes progressively more localized around $r = r_0$ as the mode number m increases. These features are seen also in the KH eigenfunctions calculated with CASTOR-FLOW [5] in Refs. 3.

The dispersion relation for the KH like instability in the step model equilibrium in Fig. 1 can be obtained after integration of Eq. (1) across $r = r_0$ and calculating also the coefficient C_+ in Eq. (1) from [6]

$$C_+ = -\frac{\Lambda_{m,n}m^2R_0^2}{n^2r_1^{2m+2}}\int_0^{r_1} r^{m+1}\frac{d\tilde{\beta}_0}{dr}\xi_{m,n}dr \tag{4}$$

where $\Lambda_{m,n} = (m+1)\,(m+2+C)/(2m-2C)$, $C = r_1\xi'_{m+1,n}/\xi_{m+1,n}$ and $\xi_{m+1,n}$ is the amplitude of the side-band $m+1$ in the edge region of the plasma. It turns out that the KH

instability appears in the regime $\widehat{\Omega}_0 \sim \mathcal{M} \gtrsim 1$, where $\widehat{\Omega}_0 = \Omega_0/\varepsilon_a\omega_A$ and $\varepsilon_a = a/R_0$ [6]. Analytical insight into parameter dependences of the eigenvalue $\omega = \omega_r + i\gamma$ can therefore be obtained from an asymptotic expansion of ω for $\widehat{\Omega}_0 \gg 1$. From the dispersion relation one obtains after some algebra the frequency and growth rate (also normalised with $\varepsilon_a\omega_A$) as [6]

$$\widehat{\omega}_r = -\frac{n(1-\lambda)}{2}\widehat{\Omega}_0 + \frac{n}{m\chi\widehat{\Omega}_0} + O\left(\frac{1}{\widehat{\Omega}_0^3}\right) \tag{5a}$$

$$\hat{\gamma}^2 = \frac{\chi(1-\lambda)}{2}\widehat{\Omega}_0^4 + \frac{(1-\lambda)[(1+\lambda)n^2+2m-8]}{4}\widehat{\Omega}_0^2 + \frac{2m(1+\lambda)+1}{2q_r^2\chi} - \Gamma\hat{\beta} - n^2\left(\frac{\widehat{\Delta q}}{q_r}\right)^2 + O\left(\frac{1}{\widehat{\Omega}_0^2}\right) \tag{5b}$$

where $\chi = (m-1)/\hat{\beta} + \lambda\Lambda_{m,n}(a/r_1)^2\, m^3/n^2$, $\hat{\beta} = \beta/\varepsilon_a^2$ and $\widehat{\Delta q} = (q_0 - q_r)/\varepsilon_a$.

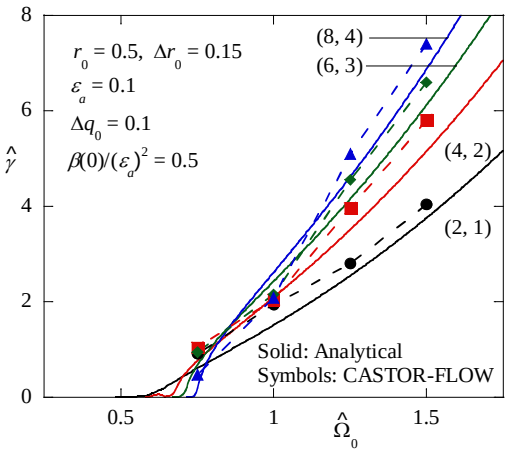

Fig. 2. *Growth rates for several (2n.n) modes obtained analytically and with CASTOR-FLOW in the equilibrium given by Eqs. (6).*

Results In Fig. 2 the growth rate for $(2n, n)$ modes is shown for a plasma with $\varepsilon_a = 0.1$ and the profiles

$$\Omega(r) = \frac{1}{2}\Omega_0 + \frac{1}{2}\Omega_0 \tanh[(r_0^2 - r^2)/(\Delta r_0)^2] \tag{6a}$$
$$p_0(r) = p_0(0)[1 - (r/a)^2]^2 \tag{6b}$$
$$\rho_0(r) = \rho_0(0)[1 - (r/a)^6] \tag{6c}$$
$$q(r) = q_0 + 2(r/a)^8 \tag{6d}$$

where $r_0 = 0.5a$, $\Delta r_0 = 0.15a$, $\hat{\beta}(0) = 0.5$ and $q_0 = 2.1$. The solid curves are calculated from Eqs. (1)-(2) and (4) while the symbols indicate CASTOR-FLOW results. The KH like instability for these mode numbers has a threshold rotation frequency of order $\widehat{\Omega}_{0,crit} \sim 0.5$-$0.8$, and the growth rate scales as $\hat{\gamma} \sim \widehat{\Omega}_0^2$ above the threshold, according to Eq. (5b). Furthermore, the growth rate scales with n as $\hat{\gamma} \sim n^{1/2}$ above the threshold, a property seen also in the numerical results of Ref. 3. Near the threshold, however, the stabilising effect of the the $n^2\Delta q$-term in Eq. (5b) becomes important. Thus, modes with large n usually have larger threshold frequencies than modes with small n, in spite of the increasing growth rates with increasing n at large $\widehat{\Omega}_0$. This property can be seen both in the analytical and the numerical solutions in Fig. 2.

Due to the stabilising Δq term in Eq. (5b), a larger Δq results in a higher threshold frequency for destabilisation of a given KH mode (m, n). This is illustrated in Fig. 3 for the (1,1) mode in the same equilibrium as in Fig. 2, but with $q_0 = 1.1, 1.2, 1.3$, and 1.4. The solid curves are again calculated from Eqs. (1) and (4) while the dashed curves are obtained from Eq. (5b). The threshold rotation frequencies $\widehat{\Omega}_{0,crit}$ obtained from CASTOR-FLOW are also indicated in the figure. Thus, the magnitude of Δq is seen to have an effect on the threshold and the growth rate near the threshold, but the effect is wiped out above the threshold by the destabilising effect from the largest, Δq-independent, term in Eq. (5b). This leads to a growth rate independent of Δq in the low-shear region when $\widehat{\Omega}_0 \gg \widehat{\Omega}_{0,crit}$, as can be seen in Fig. 3. Furthermore, unless the plasma beta is very small, the growth rate is also almost independent

of the beta value in this regime, as shown in Fig. 4 for a $(5,2)$ mode in the same equilibrium as in Figs. 2 and 3, but with $q_0 = 2.6$ and $\hat{\Omega}_0 = 2$. In this regime $\hat{\gamma} \sim \chi^{1/2}\hat{\Omega}_0^2$, and when beta is

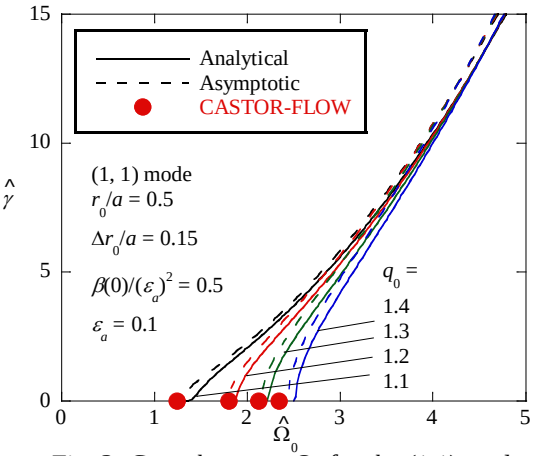

Fig. 3. *Growth rate vs* $\hat{\Omega}$ *for the (1,1) mode obtained analytically and from Eq. (5b) for the parameters indicated. Threshold rotation frequencies obtained from CASTOR-FLOW.*

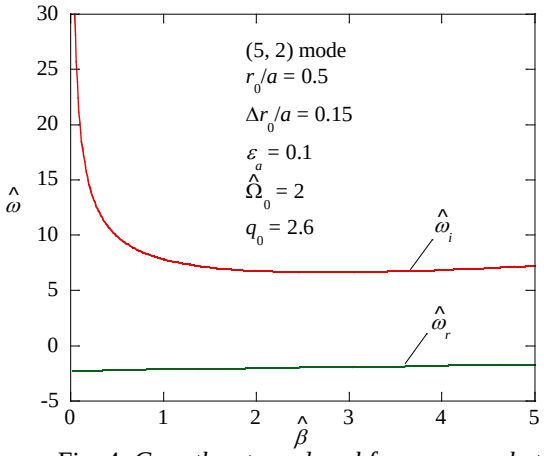

Fig. 4. *Growth rate and real frequency vs beta for the (5,2) mode obtained from the analytical model in Eqs. (1) and (4) for the parameters indicated.*

sufficiently large, χ is dominated by the $\hat{\beta}$-independent $\Lambda_{m,n}$ term, leading to the practically constant growth rate for $\hat{\beta} \gtrsim 1$ seen in Fig. 4. A similar beta dependence of the KH growth rate was seen also in the numerical results of Ref. 3.

We see that, for $\hat{\Omega}_0 \gg \hat{\Omega}_{0,crit}$, the growth rate of the KH like instability can be expressed as $\gamma^2 \sim \Lambda_{m,n} \times (\text{dynamical pressure drop})^2$, and the result comes from the C_+ term in Eq. (1). This is analogous to the infernal or QI instability in a static plasma [1], and it is therefore possible to interpret the KH instability in this regime as an infernal or, for $m = n = 1$, a QI instability, driven by the dynamical pressure drop of the plasma flow. It is seen that instability can occur in these strongly rotation-sheared plasmas even when the value of q in the low-shear region is far from rational. Compared to a static plasma, the stabilising dependence of magnetic field line bending is weak, as is also the dependence of the static pressure.

The authors acknowledge E. Strumberger and H. P. Zehrfeld for providing them with the CASTOR-FLOW and DIVA codes. This work was partly funded by the United Kingdom Engineering and Physical Sciences Research Council and by the European Communities under the contracts of Association between EURATOM, the Swedish Research Council (VR), UKAEA and the Fonds National Suisse de la Recherche Scientifique. The views and opinions expressed herein do not necessarily reflect those of the European Commission.

References

[1] J. Manickam, N. Pomphrey and A. M. M. Todd, Nuclear Fusion **27**, 1461, 1987; R. J. Hastie and T. C. Hender, Nuclear Fusion **28**, 585, 1988; F. L. Waelbroeck and R. D. Hazeltine, Physics of Fluids **31**, 1217, 1988; C. Wahlberg and J. P. Graves, Physics of Plasmas **14**, 110703, 2007.

[2] C. Wahlberg, Plasma Physics and Controlled Fusion, **47**, 757, 2005; Proc. of the 32nd EPS Conf. on Plasma Physics, Tarragona, P4.068, 2005.

[3] I. T. Chapman, N. R. Walkden, J. P. Graves and C. Wahlberg, Plasma Physics Controlled Fusion, **53**, 125002, 2011; I. T. Chapman, S. Brown, R. Kemp and N. R. Walkden, Nucl. Fusion **52**, 042005, 2012.

[4] C. Wahlberg, Plasma Physics and Controlled Fusion, **51**, 085006, 2009.

[5] E. Strumberger, S. Günter, P. Merkel, S. Riondato, E. Schwarz, C. Tichmann and H. P. Zehrfeld, Nucl. Fusion **45**, 1156 (2005).

[6] C. Wahlberg , J. P. Graves and I. T. Chapman, paper in preparation.